Improved Energy Detector for Random Signals in Gaussian Noise

Yunfei Chen, *Member, IEEE*

***Abstract*—New and improved energy detector for random signals in Gaussian noise is proposed by replacing the squaring operation of the signal amplitude in the conventional energy detector with an arbitrary positive power operation. Numerical results show that the best power operation depends on the probability of false alarm, the probability of detection, the average signal-to-noise ratio or the sample size. By choosing the optimum power operation according to different system settings, new energy detectors with better detection performances can be derived. These results give useful guidance on how to improve the performances of current wireless systems using the energy detector. It also confirms that the conventional energy detector based on the generalized likelihood ratio test using the generalized likelihood function is not optimum in terms of the detection performance.**

***Index Terms*—Energy detector, probability of detection, probability of false alarm, spectrum sensing.**

I. Introduction

THE energy detector is a very useful non-coherent detector for signals corrupted by Gaussian noise [1]. It detects the presence of a signal by measuring its energy and comparing the measured energy with a predetermined threshold. The measurement and the comparison require no channel state information. Thus, the energy detector has a very simple structure, and it has been widely used in wireless communications systems. For example, in ultra-wide bandwidth systems with pulse position modulation, the energy detector is a good alternative to the Rake receiver [2] - [4] and the transmitted-reference receiver [5] in applications where simple receiver structures are preferred [6]- [8]. As well, in cognitive radio systems, although the energy detector underperforms the matched filtering detector and the feature-based detector [9], [10], it is often used in spectrum sensing applications where a quick sensing decision is required, as the energy detector offers great simplicity while the feature-based detector often needs a large sample size to calculate cyclostationarity, covariance or eigenvalues, and the matched filtering detector is often unrealistic. The performance of the energy detector can be further improved by adopting collaboration between different cognitive radio users [11], [12].

The original energy detector proposed in [1] dealt with the detection of an unknown deterministic signal buried in Gaussian noise. In [13] and [14], this detector has been extended to detect a random signal corrupted by Gaussian noise. However, all of these results are based on the generalized likelihood ratio test method, where the generalized likelihood function is maximized [15]. In some communications applications, the probability of erroneous detection or the probability of correct detection are of more interest. The detector that maximizes the generalized likelihood function may not be the same as the detector that maximizes the probability of correct detection or that minimizes the probability of erroneous detection. This gives motivation to an investigation of energy detectors that are better than those presented in [1], [13], [14].

In this letter, improved energy detector for random signals corrupted by Gaussian noise is derived. The derivation is based on a simple modification to the conventional energy detector in [1], [13], [14] by replacing the squaring operation of the signal amplitude with an arbitrary positive power operation. Numerical results show that the best power operation of the signal amplitude depends on the probability of false alarm, the probability of detection, the average signal-to-noise ratio (ASNR) or the sample size, but it generally does not equal to two as in the conventional energy detector.

II. Derivation

Consider a binary hypothesis testing problem with

$$\begin{aligned} H_0 : y_i &= w_i \\ H_1 : y_i &= s_i + w_i \end{aligned} \tag{1}$$

where H_0 represents the hypothesis that the signal is absent, H_1 represents the hypothesis that the signal is present, $i = 1, 2, \cdots, n$ index the n signal samples, w_i is additive white Gaussian noise with mean zero and variance σ^2, and s_i is the fading signal. In a binary pulse position modulated (BPPM) ultra-wide bandwidth (UWB) system, the bit interval is divided into two parts. If the data bit is 0, the signal will be transmitted in the first part of the bit interval. If the data bit is 1, an additional time shift will be introduced such that the signal will be transmitted in the second part of the bit interval. At the receiver, the energy of the first part is compared with that of the second part to determine the presence of the signal, and therefore, the data bit transmitted [8]. In this case, y_i in H_0 represents the received signal for the part without signal in the bit interval, while y_i in H_1 represents the received signal for the part with signal in the bit interval. In a cognitive radio system, y_i represents the signal from the primary user. Assume that the random signal follows a Gaussian distribution with mean zero and variance α^2. Also, assume that the signal samples are independent. In this letter, real signals are considered. The results can be easily extended to complex signals. As well, the noise samples w_i, $i = 1, 2, \cdots, n$, are assumed independent.

Manuscript received May 1, 2009; revised August 3, 2009 and November 3, 2009; accepted November 12, 2009. The associate editor coordinating the review of this paper and approving it for publication was A. Conti.

This work was supported in part by EPSRC First Grant under EP/F030843/1.

Y. Chen is with the School of Engineering, University of Warwick, Coventry, U.K. CV4 7AL (e-mail: Yunfei.Chen@warwick.ac.uk).

Digital Object Identifier 10.1109/TWC.2010.02.090622

From (1), the joint probability density function (PDF) of the samples can be derived as

$$p(\mathbf{y}|H_0) = \frac{1}{\left(\sqrt{2\pi\sigma^2}\right)^n} e^{-\frac{\sum_{i=1}^n y_i^2}{2\sigma^2}} \tag{2}$$

under H_0 and

$$p(\mathbf{y}|H_1, \mathbf{s}) = \frac{1}{\left(\sqrt{2\pi\sigma^2}\right)^n} e^{-\frac{\sum_{i=1}^n (y_i - s_i)^2}{2\sigma^2}} \tag{3}$$

under H_1, conditioned on the unkown signal amplitudes $\mathbf{s}$, where $\mathbf{y} = [y_1 \quad y_2 \quad \cdots y_n]$ and $\mathbf{s} = [s_1 \quad s_2 \quad \cdots s_n]$. Using the generalized likelihood ratio test approach together with the Gaussian distribution of s_i, the conventional energy detector can be derived as [13], [14]

$$W = \frac{1}{n}\sum_{i=1}^n \left(\frac{y_i}{\sigma}\right)^2 \underset{H_0}{\overset{H_1}{\gtrless}} T \tag{4}$$

where the signal sample y_i is normalized with respect to the noise standard deviation and then squared, and T is the detection threshold to be determined. Using (4), the PDF of W under H_0 can be shown to follow a chi-square distribution or a Gamma distribution

$$p_{W|H_0}(x) = \frac{1}{\theta_0^{k_0}\Gamma(k_0)} x^{k_0-1} e^{-\frac{x}{\theta_0}}, \quad x \geq 0 \tag{5}$$

with shape parameter $k_0 = \frac{n}{2}$ and scale parameter $\theta_0 = \frac{2}{n}$, and the PDF of W under H_1 also follows a Gamma distribution

$$p_{W|H_1}(x) = \frac{1}{\theta_1^{k_1}\Gamma(k_1)} x^{k_1-1} e^{-\frac{x}{\theta_1}}, \quad x \geq 0 \tag{6}$$

with shape parameter $k_1 = \frac{n}{2}$ and scale parameter $\theta_1 = \frac{2}{n}(1+\gamma)$, where $\Gamma(\cdot)$ denotes the complete Gamma function and $\gamma = \frac{\alpha^2}{\sigma^2}$ is the ASNR [13], [14]. Denote

$$P_F = Pr\{W > T|H_0\} \tag{7}$$

as the probability of false alarm and

$$P_D = Pr\{W > T|H_1\} \tag{8}$$

as the probability of detection. The receiver operating characteristics (ROC) curve is the most important performance measure for a hypothesis testing problem. It describes the relationship between P_F and P_D. Using (5) in (7), the detection threshold can be determined according to the Neyman-Pearson rule as

$$T = F_{W|H_0}^{-1}(1 - P_F, k_0, \theta_0) \tag{9}$$

and the ROC curve for the conventional energy detector can be derived using (6) and (9) in (8) as

$$\begin{aligned} P_D &= 1 - F_{W|H_1}(T, k_1, \theta_1) \\ &= 1 - F_{W|H_1}(F_{W|H_0}^{-1}(1 - P_F, k_0, \theta_0), k_1, \theta_1) \end{aligned} \tag{10}$$

where $F_{W|H_1}(x, k_1, \theta_1) = \int_0^x \frac{1}{\theta_1^{k_1}\Gamma(k_1)} t^{k_1-1} e^{-\frac{t}{\theta_1}} dt$ is the cumulative distribution function (CDF) of a Gamma distribution with shape parameter k_1 and scale parameter θ_1, and $F_{W|H_0}^{-1}(x, k_0, \theta_0)$ is the inverse function of $F_{W|H_0}(x, k_0, \theta_0) = \int_0^x \frac{1}{\theta_0^{k_0}\Gamma(k_0)} t^{k_0-1} e^{-\frac{t}{\theta_0}} dt$ with shape parameter k_0 and scale parameter θ_0. The detector in (4) maximizes the generalized likelihood function, as can be seen from [15, eq. (7.2)], but it doesn't necessarily minimize the probability of false alarm or maximize the probability of detection in (10).

In order to improve the detection performance of the conventional energy detector, in this letter, a new energy detector is proposed as

$$W' = \frac{1}{n}\sum_{i=1}^n \left(\frac{|y_i|}{\sigma}\right)^p \underset{H_0}{\overset{H_1}{\gtrless}} T' \tag{11}$$

where $p > 0$ is an arbitrary constant and T' is the detection threshold to be determined. Thus, the only difference between (4) and (11) is that the squaring operation in (4) is replaced by an arbitrary positive power operation of p in (11) and that the detection threshold is changed accordingly. One sees that the conventional energy detector is a special case of the new energy detector when $p = 2$. In this case, the decision variable W' doesn't follow a Gamma distribution in general. However, as will be shown later, W' can be well approximated as a Gamma random variable by matching the mean and the variance. This approximation enables us to determine the detection threshod T' for the new detector in (11), which is otherwise difficult to obtain without the distribution of W'. Using [16, eq. 3.462.9], one has the mean and the variance of W' as

$$\begin{aligned} E\{W'|H_0\} &= \frac{2^{p/2}}{\sqrt{\pi}}\Gamma\left(\frac{p+1}{2}\right) \\ Var\{W'|H_0\} &= \frac{2^p\Gamma\left(\frac{2p+1}{2}\right)}{n\sqrt{\pi}} - \frac{2^p}{n\pi}\Gamma^2\left(\frac{p+1}{2}\right) \end{aligned} \tag{12}$$

under H_0, and the mean and the variance of W' as

$$\begin{aligned} E\{W'|H_1\} &= \frac{2^{p/2}}{\sqrt{\pi}}\Gamma\left(\frac{p+1}{2}\right)\left(\sqrt{1+\gamma}\right)^p \\ Var\{W'|H_1\} &= \frac{2^p(1+\gamma)^p\Gamma\left(\frac{2p+1}{2}\right)}{n\sqrt{\pi}} \\ &\quad - \frac{2^p(1+\gamma)^p}{n\pi}\Gamma^2\left(\frac{p+1}{2}\right) \end{aligned} \tag{13}$$

under H_1. Using (12) and (13) in a Gamma approximation, one has the PDF of W' under H_0 as a Gamma distribution given in (5) but with shape parameter and scale parameter

$$\begin{aligned} k_0' &= \frac{E^2\{W'|H_0\}}{Var\{W'|H_0\}} = n \cdot \frac{\Gamma^2\left(\frac{p+1}{2}\right)}{\Gamma\left(\frac{2p+1}{2}\right)\sqrt{\pi} - \Gamma^2\left(\frac{p+1}{2}\right)} \\ \theta_0' &= \frac{Var\{W'|H_0\}}{E\{W'|H_0\}} = \frac{2^{p/2}}{n} \cdot \frac{\sqrt{\pi}\Gamma\left(\frac{2p+1}{2}\right) - \Gamma^2\left(\frac{p+1}{2}\right)}{\Gamma\left(\frac{p+1}{2}\right)\sqrt{\pi}} \end{aligned} \tag{14}$$

and the PDF of W' under H_1 as a Gamma distribution given

in (6) but with shape parameter and scale parameter

$$\begin{aligned} k_1' &= \frac{E^2\{W'|H_1\}}{Var\{W'|H_1\}} \\ &= n \cdot \frac{\Gamma^2\left(\frac{p+1}{2}\right)}{\Gamma\left(\frac{2p+1}{2}\right)\sqrt{\pi} - \Gamma^2\left(\frac{p+1}{2}\right)} \\ \theta_1' &= \frac{Var\{W'|H_1\}}{E\{W'|H_1\}} \\ &= \frac{2^{p/2}(1+\gamma)^{p/2}}{n} \cdot \frac{\sqrt{\pi}\Gamma\left(\frac{2p+1}{2}\right) - \Gamma^2\left(\frac{p+1}{2}\right)}{\Gamma\left(\frac{p+1}{2}\right)\sqrt{\pi}}. \end{aligned} \quad (15)$$

Finally, using (14) and (15), one has a closed-form expression for the detection threshold as

$$T' = F^{-1}_{W'|H_0}(1 - P_F, k_0', \theta_0') \quad (16)$$

and the ROC curve for the new detector as

$$\begin{aligned} P_D &= 1 - F_{W'|H_1}(T', k_1', \theta_1') \\ &= 1 - F_{W'|H_1}(F^{-1}_{W'|H_0}(1 - P_F, k_0', \theta_0'), k_1', \theta_1') \end{aligned} \quad (17)$$

where $F_{W'|H_1}(\cdot,\cdot,\cdot)$ and $F^{-1}_{W'|H_0}(\cdot,\cdot,\cdot)$ are similar to $F_{W|H_1}(\cdot,\cdot,\cdot)$ and $F^{-1}_{W|H_0}(\cdot,\cdot,\cdot)$ defined before, respectively, except that k_0, k_1, θ_0 and θ_1 in $F_{W|H_1}(\cdot,\cdot,\cdot)$ and $F^{-1}_{W|H_0}(\cdot,\cdot,\cdot)$ are replaced by k_0', k_1', θ_0' and θ_1' given in (14) and (15) in this case. One sees that the value of p is implicitly related to the probability of false alarm P_F, the probability of detection P_D, the ASNR γ, and the sample size n through (17). One can find the optimum value of p that maximizes the probability of detection by using (17) at fixed values of P_F, γ and n. Then, the value of p that achieves the maximum probability of detection is a function of P_F, γ and n. One can also find the optimum value of p that minimizes the probability of false alarm by using (17) at fixed values of P_D, γ and n. Then, the value of p that achieves the minimum probability of false alarm is a function of P_D, γ and n. As well, one can find the optimum value of p that minimizes the sample size n by using (17) at fixed values of P_F, P_D and γ. Then, the value of p that achieves the minimum sample size is a function of P_D, P_F and γ. Thus, (17) is a very general expression that can be used in different applications. An analytical expression for the optimum value of p is difficult to obtain, if not impossible. In the next section, the optimum values of p will be examined at different parameters of P_F, P_D, γ or n through numerical calculations.

III. Numerical Results and Discussion

In this section, the performances of the conventional energy detector and the improved energy detector are compared. In order to conduct the comparison, the accuracy of the Gamma approximation to the CDF of W' is verified by simulation first. Then, the optimum values of p are determined.

Figs. 1 and 2 compare the simulated CDF of W' with the Gamma approximate CDF of W' under H_0 and H_1, respectively. The simulated CDF is obtained by using the MATLAB function 'ecdf'. One sees from Figs. 1 and 2 that the Gamma approximation works well in most cases considered. The accuracy of the approximation increases when p decreases, n increases or γ decreases. The value of the

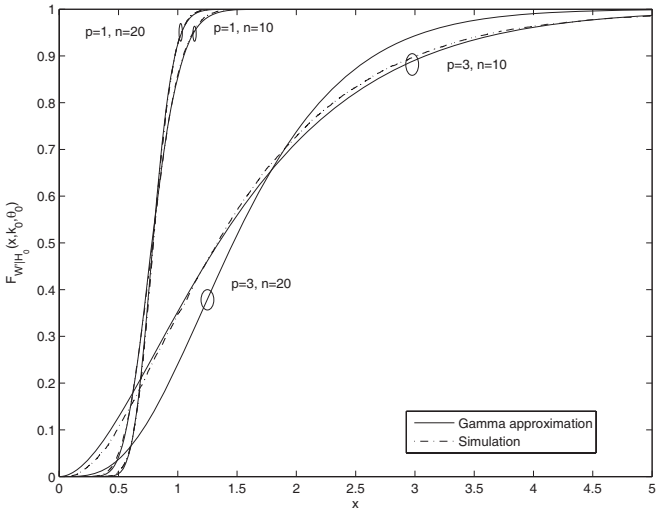

Fig. 1. Comparison of the simulated CDF and the Gamma approximation for W' under H_0 when $\gamma = 0\ dB$.

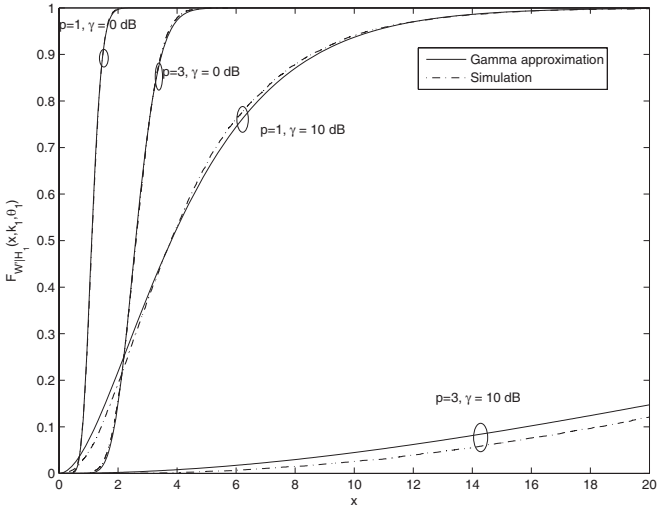

Fig. 2. Comparison of the simulated CDF and the Gamma approximation for W' under H_1 when $n = 10$.

ASNR γ has the largest effect on the approximation error. Since practical ultra-wide bandwidth systems often operate at a low SNR to achieve low power consumption and the licensed user's signal is usually weak in cognitive radio systems, the accuracy of the Gamma approximation may be enough for practical energy detectors. Moreover, this accuracy can be improved by using more signal samples in the detection.

Fig. 3 shows the optimum value of p that maximizes the probability of detection vs. P_F for different fixed values of γ and n, based on (17). The value of p is tested from 0.01 to 10 with a step size of 0.01. From Fig. 3, one sees that the optimum value of p decreases as P_F increases. The rate of the decrease is approximately constant when P_F is small. However, when P_F is approaching 1, the optimum value of p drops quickly. One also sees that, when $\gamma = 10\ dB$, none of the optimum values of p equal to two, corresponding to the conventional energy detector. When $\gamma = 0\ dB$, the optimum value of p equals to two for $P_F = 10^{-1}$. From (7), the

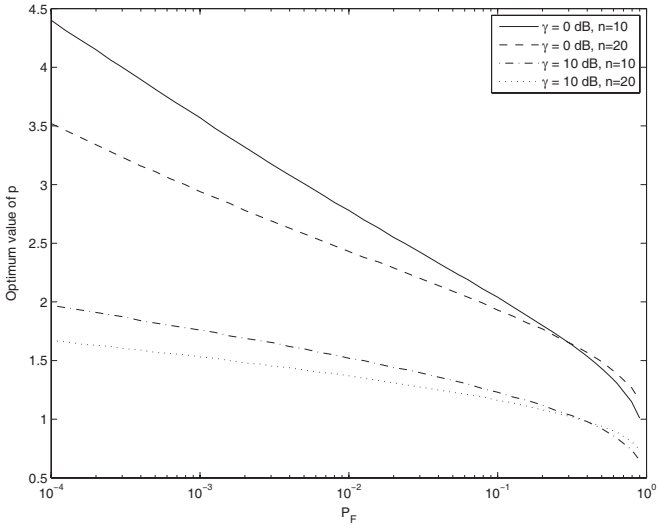

Fig. 3. The optimum value of p that maximizes the probability of detection vs. P_F for different fixed values of γ and n.

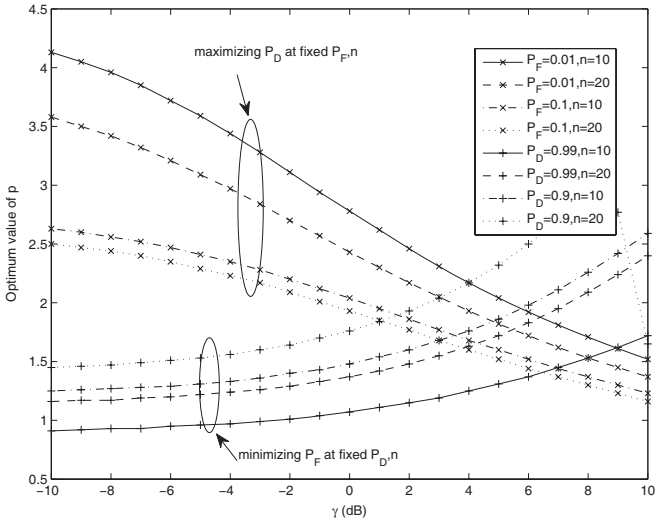

Fig. 4. The optimum value of p maximizing the probability of detection vs. γ for different fixed values of P_F and n, as well as the optimum value of p minimizing the probability of false alarm vs. γ for different fixed values of P_D and n.

value of P_F is the probability that the cognitive radio decides that the licensed band is occupied while it is actually free. This represents a missed opportunity for the cognitive radio to transmit its data in the licensed band. From the cognitive radio's perspective, P_F should be set as small as possible and $P_F = 10^{-1}$ may be too high in practice. Thus, practical values of P_F may be less than 10^{-1} and the optimum p doesn't equal to two in these cases either. One concludes from Fig. 3 that the conventional energy detector doesn't give the maximum probability of detection in most cases considered. Fig. 4 shows the optimum value of p that maximizes the probability of detection vs. γ for different fixed values of P_F and n, as well as the optimum value of p that minimizes the probability of false alarm vs. γ for different fixed values of P_D and n, based on (17). From Fig. 4, one sees that the optimum value of p maximizing P_D decreases as γ increases, and the rate

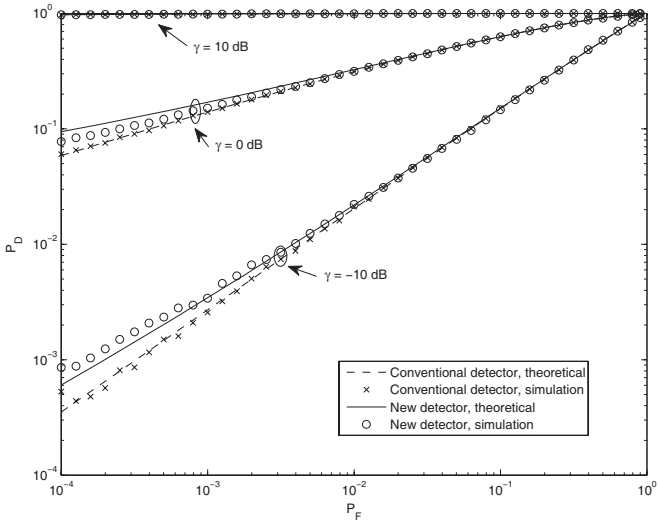

Fig. 5. Comparison of the ROCs for the conventional energy detector and the new energy detector when $n = 10$ for different values of γ.

of the decrease is higher at small values of γ than that at large values of γ. On the other hand, the optimum value of p minimizing P_F increases as γ increases in most cases, and the rate of the increase is lower at small values of γ than that at large values of γ. The optimum value of p maximizing P_D approaches some common floor when γ is large, while the optimum value of p minimizing P_F approaches some common floor when γ is small. Again, in most cases, the optimum value of p doesn't equal to two as in the conventional energy detector. One concludes from Figs. 3 and 4 that the optimum value of p depends on P_F, P_D, γ or n. In practical systems, P_F, P_D and n are often predetermined. The value of γ can be estimated using SNR estimation methods proposed in [17] and [18], depending on the system structures. Using the known P_F, P_D, n and the estimated γ, together with graphs similar to Figs. 3 and 4, one can determine the optimum value of p for operation in the new energy detector.

Fig. 5 compares the ROC curve of the conventional energy detector with that of the new energy detector with optimized p from (17). The theoretical results for the conventional and new energy detectors are obtained by using (10) and (17), respectively. The simulation results for the conventional and new energy detectors are obtained by using (9) and (16) in (4) and (11), respectively. One sees that the new energy detector with optimized p outperforms the conventional energy detector in all the cases considered. However, this is not obvious for $\gamma = 10\ dB$, where the difference between the conventional energy detector and the new energy detector is graphically negligible. The performance gain increases as the probability of false alarm decreases, and it is significant when P_F is less than or equal to 10^{-3}. This implies that one may choose P_F to be smaller than or equal to 10^{-3} in order to achieve significant gain by using the optimized energy detector, or one may choose P_F to be larger than 10^{-3} in order to avoid significant loss by using the conventional energy detector. One also sees that the theoretical performance gain from the Gamma approximation overestimates the simulated performance gain from the true distribution when $\gamma = 0\ dB$,

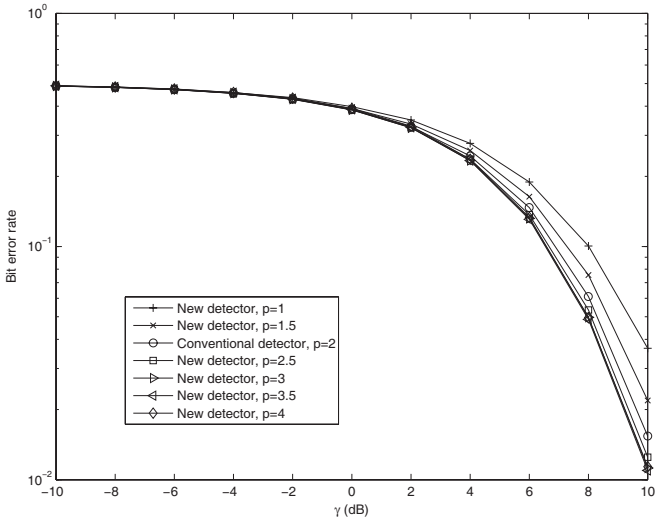

Fig. 6. Comparison of the bit error rates for the conventional energy detector and the new energy detector using different fixed values of p for a BPPM UWB system in the IEEE CM1 channel.

while it underestimates the simulated performance gain when $\gamma = -10\ dB$, at small values of P_F. This is mainly caused by the approximation errors in (14) and (15), which give values of p that optimize (17) but not necessarily the true performance. However, it is crucial to apply approximation to the distribution of W' in order to derive the threshold T' for detection. One may use more accurate approximations to the distribution of W' to reduce the approximation errors. The performance gain always exists, even using a fixed non-optimized p in some cases, as will be shown later. In the case of low operating ASNR, the theoretical performance gain may be considered as a lower bound of the true gain.

Fig. 6 shows the bit error rate performance of the new energy detector for a BPPM UWB system using the IEEE CM1 channel model [21]. In the simulation, the pulse duration is set to 2 ns, while the additional time shift is set to 100 ns and the bit interval is set to 200 ns to avoid intersymbol interferences, as the energy detector is often used in UWB applications where reliability is more important than the data rate [6] - [8]. A second-order Gaussian monocycle is used. The number of channel realizations tested is 250, and the number of data bits tested is 1000. Unlike the new energy detector in Fig. 5 that uses the optimized p for each ASNR value, in Fig. 6, a fixed p is tested for all the values of SNR. Thus, the result is not based on (17), and it doesn't depend on the approximation accuracy. One sees that, when γ is less than 0 dB, the performance difference is negligible. However, when γ is larger than 0 dB, the larger the value of p is, the better the new energy detector will perform. The conventional energy detector has a larger bit error rate than the new energy detector with p fixed at 2.5 to 4. Thus, the new energy detector outperforms the conventional energy detector even when a fixed p is used without any knowledge of the ASNR to determine the optimum p. The conventional energy detector is based on the maximization of the generalized likelihood function, as can be seen from [15, eq. (7.2)], while the new energy detector is based on the maximization of the probability of detection or the minimization of the probability of false alarm, as can be seen from (17). Figs. 3 - 6 in this letter prove that they are not the same in general.

The purpose of this letter is to reduce the performance gap between the conventional non-coherent energy detector and the coherent detector. This can be achieved by trying something between the generalized likelihood function and the decision variable. In this letter, instead of taking a squaring operation over the received sample, one takes an arbitrary positive power operation. In this sense, the idea is *ad hoc*. However, the obtained results are still encouraging. The performance gain of the new energy detector over the conventional energy detector might be caused by the fact that a squaring operation may understate the signal component in the sample when the SNR is large and overstate the signal component in the sample when the SNR is small. The above results show that changing the squaring operation to an arbitrary positive power operation is effective in improving the performance of the conventional energy detector. Interestingly, similar methods have also been used in equalization and power control to achieve better performances [19], [20].

IV. Conclusion

The detection performance of the conventional energy detector has been improved by choosing the value of the power operation of the signal sample according to the system settings. Numerical results have shown that the optimum power operation depends on the probability of false alarm, the ASNR as well as the sample size. Using the relationships between the optimum power operation and the probability of false alarm, the ASNR and the sample size, new energy detectors that outperform the conventional energy detector have been derived. Future works include examination of other non-linear forms of the signal samples to improve the detection performance of the energy detector further.

References

[1] H. Urkowitz, "Energy detection of unknown deterministic signals," *Proc. IEEE*, vol. 55, pp. 523-531, Apr. 1967.
[2] D. Cassioli, M. Z. Win, F. Vatalaro, and A. F. Molisch, "Low complexity Rake receivers in ultra-wideband channels," *IEEE Trans. Wireless Commun.*, vol. 6, pp. 1265-1275, Apr. 2007.
[3] M. Z. Win and R. A. Scholtz, "Impulse radio: how it works," *IEEE Commun. Lett.*, vol. 2, pp. 36-38, Feb. 1998.
[4] M. Z. Win and R. A. Scholtz, "Ultrawide bandwidth time-hopping spread-spectrum impulse radio for wireless multiple-access communications," *IEEE Trans. Commun.*, vol. 48, pp. 679-691, Apr. 2000.
[5] T. S. Quek and M. Z. Win, "Analysis of UWB transmitted-reference communication systems in dense multipath channels," *IEEE J. Sel. Areas Commun.*, vol. 23, pp. 1863-1874, Sep. 2005.
[6] E. Arias-de-Reyna, A. A. D'Amico, and U. Mengali, "UWB energy detection receivers with partial channel knowledge," in *Proc. IEEE ICC 2006*, vol. 10, pp. 4688-4693, Istanbul, Turkey, 2006.
[7] M. Weisenhorn and W. Hirt, "Robust noncoherent receiver exploiting UWB channel properties," in *Proc. IEEE UWBST*, Kyoto, Japan, May 2004.
[8] C. Carbonelli and U. Mengali, "M-PPM noncoherent receivers for UWB applications," *IEEE Trans. Wireless Commun.*, vol. 5, pp. 2285-2294, Aug. 2006.
[9] D. Cabric, S. M. Mishra, and R. W. Brodersen, "Implementation issues in spectrum sensing for cognitive radios," in *Proc. IEEE Asilomar Conference on Signals, Systems and Computers 2004*, pp. 772-776, Pacific Grove, CA, USA, Nov. 2004.
[10] M. Ghozzi, M. Dohler, F. Marx, and J. Palico, "Cognitive radios: methods for detection of free bands," *Elsevier Science J.*, special issue on cognitive radio, vol. 7, pp. 794-805, Sep. 2006.

[11] Y. Chen and N. C. Beaulieu, "Performance of collaborative spectrum sensing for cognitive radio in the presence of Gaussian channel estimation errors," *IEEE Trans. Commun.*, vol. 57, pp. 1944-1947, July 2009.

[12] E. Visotsky, S. Kuffner, and R. Peterson, "On collaborative detection of TV transmissions in support of dynamic spectrum sharing," in *Proc. IEEE DySPAN 2005*, pp. 338-345, Baltimore, U.S.A., Nov. 2005.

[13] V. I. Kostylev, "Energy detection of a signal with random amplitude," in *Proc. ICC 2002*, New York, pp. 1606-1610, May 2002.

[14] F. F. Digham, M.-S. Alouini, and M. K. Simon, "On the energy detection of unknown signals over fading channels," *IEEE Trans. Commun.*, vol. 55, pp. 21-24, Jan. 2007.

[15] S. M. Kay, *Fundamentals of Statistical Signal Processing: Detection Theory*. Upper Saddle River, NJ: Prentice-Hall, 1998.

[16] I. S. Gradshteyn and I. M. Ryzbik, *Table of Integrals, Series, and Products*, 6th ed. San Diego, CA: Academic Press, 2000.

[17] Y. Chen and N. C. Beaulieu, "SNR estimation methods for UWB systems," *IEEE Trans. Wireless Commun.*, vol. 6, pp. 3836-3845, Oct. 2007.

[18] Y. Chen and N. C. Beaulieu, "Maximum likelihood estimation of SNR using digitally modulated signals," *IEEE Trans. Wireless Commun.*, vol. 6, pp. 210-219, Jan. 2007.

[19] A. Conti, B. Masini, F. Zabini, and O. Andrisano, "On the down-link performance of multi-carrier CDMA systems with partial equalization," *IEEE Trans. Wireless Commun.*, vol. 6, pp. 230-239, Jan. 2007.

[20] M. Chiani, A. Conti, and R. Verdone, "Partial compensation signal-level-based up-link power control toextend terminal battery duration," *IEEE Trans. Veh. Technol.*, vol. 50, pp. 1125-1131, July 2001.

[21] "Channel modeling sub-committee report final," IEEE P802.15-02/490r1-SG3a, Feb. 2003.